

# Nearshore propagation of cyclonic waves

J. K. Panigrahi · P. A. Umesh · C. P. Padhy · J. Swain

Received: 10 November 2009 / Accepted: 2 November 2011 / Published online: 1 December 2011  
© Springer Science+Business Media B.V. 2011

**Abstract** Cyclone-generated surface waves are simulated using state-of-art SWAN (Simulating Waves Nearshore) model coupled with hydrodynamic model inputs. A severe cyclonic storm passed over the Arabian Sea during 4–9th November 1982 is selected from UNISYS track records. The cyclone lasted for nearly 6 days and subsided with a land fall at Gujarat coast, west coast of India. In this study, cyclonic wind fields are generated using a well-established relationship suggested by Jelesnianski and Taylor (1973). The associated water level variations due to storm surge and surge generated currents are simulated using POM (Princeton Ocean Model). The outputs are one-way coupled with the wave model SWAN for simulating wave parameters off Gujarat, north-east basin of Arabian Sea. An extensive literature review is carried out on the progress and methodology adopted for storm wave modelling and analysis. The results presented in this paper reveal the severity of the storm event and would be highly useful for assessing the extreme wave event/climate especially for the south coast of Gujarat.

**Keywords** Wave prediction · Wave simulation · Cyclonic wave modelling · Extreme wave · SWAN

## 1 Introduction

The phenomenal generation of ocean waves from a cyclone depends on a number of atmospheric, meteorological and oceanographic factors and hence becomes very complex

---

J. K. Panigrahi (✉)  
Department of Marine Science, Berhampur University, Berhampur, India  
e-mail: Jeetendra@scientist.com

P. A. Umesh · J. Swain  
Naval Physical and Oceanographic Laboratory, Kochi 21, India

C. P. Padhy  
Department of Ocean Engineering and Naval Architecture,  
Indian Institute of Technology, Kharagpur 2, India

to describe mathematically. The physics of wave generation by cyclones is complicated due to rapidly turning winds that generate cross-seas and hence changes wind speed and direction with space (cyclone location) and time. Cyclonic wind fields are characteristically intense, spatially inhomogeneous and directionally varying. The large gradients in wind speed and the rapidly varying wind directions of the storm vortex generate complex ocean waves. Typically, waves generated by cyclones consist of combined wind-seas and swells. In addition, the directional distribution of the wind-sea component is often skewed due to the rapid variation in the wind direction. Complexity of the wave generation process within the cyclone wind field provides a challenging demand to test the capability of the wind and wave prediction models. However, the third generation numerical wave models like WAM (WAVE Model, WAMDI group 1988) and SWAN (Simulating WAVes Near-shore, Booij et al. 1999) based on the energy balance equation by incorporating the latest physics of wave generation became popular in the 1990s due to their mathematical rigour and also owing to a large temporal and spatial coverage yielded by these models in addressing the rapidly varying cyclonic waves to a greater extent. Cyclonic wave is an important input parameter for planning and safe design of ocean structures in tropical and semi-tropical regions. The extreme waves are generated by the cyclonic disturbances and propagate to the coastal and nearshore waters. Their wave heights are exceptionally high in the shallow waters, and the wave characteristics change from storm to storm. The simultaneous generation of storm surge and the surge generated currents has very significant impact on wave propagation in shallow waters due to such varying hydrodynamics. In addition, deep-water waves that may be generated and propagating from different locations as well as directions during any given storm are generally affected by refraction, diffraction, reflection and shoaling in shallow waters. In this context, a detailed review on the advancement of research on cyclonic waves is illustrated in this paper. Most importantly, a simulation experiment is carried out to assess the applicability of SWAN model for cyclonic system and its suitability for engineering decision making is discussed. SWAN is implemented in non-stationary mode taking into account of wave propagation by considering the POM (Princeton Ocean Model, Mellor 1996)-simulated variable surge levels and surface currents during the passage of a cyclone considered.

## 2 Cyclone-generated waves: a review

Waves generated by cyclones can exceed as high as 10–20 m in the open ocean (deep waters). Wang et al. (2005) reported that the maximum significant wave height was 27.7 m during the passage of Hurricane Ivan. Although, significant wave height is lower when waves reach shallow waters, these waves can devastate the coastal zone. It is well known that hurricane-induced waves are one of the most devastating phenomena during the passages of hurricanes. Moreover, severe wave conditions are dangerous to ocean going vessels and waves may also run up with the occurrence of storm surge in the coastal zone causing more severe damages along as well as landward limits of the coast. Therefore, the ability to precisely predict the hurricane-induced waves is a very important challenge and is of greater importance to many user communities. The wind being the principal source of energy for the generation and growth of waves, in order to forecast the hurricane-induced ocean surface waves, it is necessary to establish a thorough understanding of how the wave field manifests itself in response to the spatial and temporal variations of hurricane winds. In this regard, the available literature on the subject has been reviewed and the important highlights or the research findings are presented.

In fifties, the theories of energy transfer (Phillips 1957) from wind to wave and their feedback mechanisms (Miles 1957) were well developed. The wave models such as WAM and SWAN are still using the theories of Phillips and Miles. These two wave models have been thoroughly validated and extensively used to forecast, nowcast and hindcast waves incorporating wave–current interactions, and their results are analysed over various parts of global oceans (Komen et al. 1994; Xie et al. 2001; Booij et al. 1999; Ris et al. 1999). There are a number of studies that are referred in this paper on the response of wind-waves to tropical cyclones. Wright et al. (2001) and Walsh et al. (2002) have provided all quadrants of sea surface directional wave spectrum in the open ocean (August 24, 1998) and at landfall (August 26, 1998) during the passage of hurricane Bonnie based on the analysis of NASA airborne scanning radar altimeter data. They have concluded that the dominant waves generally propagate at significant angles to the down wind direction and have developed a simple model to predict the predominant wave propagation direction. Recently, Young (2006) studied the directional wave spectrum during the passage of several hurricanes using wave buoy observations and established the fact that in all quadrants of the storm, the dominant waves are remotely generated swells. A study by Ou et al. (2002) on SWAN-simulated typhoon waves in the coastal waters of Taiwan revealed the significance of typhoon-induced waves in the study area. Their results also indicate that waves under hurricane forcing can be reasonably simulated by SWAN wave model. Similarly, Moon et al. (2003) have simulated the surface wave spectra under hurricane wind forcing using a high-resolution WAVEWATCH III model (Tolman 1991). They found that numerical simulation results agree reasonably well with the observations. Further, they analysed the effect of hurricane translation speed on the wave spectra. However, their study focused or limited to analysis of a specific case. Among the other investigations, the study by Moon et al. (2004) is pertinent to mention here as they investigated the importance of sea surface waves on air–sea momentum flux during the passages of tropical cyclones.

Cyclone translation to wave is a growing field of research and many latest publications on this subject (Fan et al. 2009a, b) reveal newer findings. Author's latest work (Panigrahi and Misra 2009) describes on the delineation of fetch from a hurricane and the numerical hindcast of extreme waves using Young's parametric wave model (Young 1988). In spite of several such research efforts, the direction of propagation of swells with respect to a storm/hurricane track is still nebulous. Figure 1 shows the schematic of swell (of Point A and Point B) propagating in a direction tangential to the circle defined by the radius to maximum wind, an earlier position of the storm. This picture (Moon et al. 2003) is based on the assumption that the swells are generated from the earlier position of the storm, and their propagation direction at each point is determined by the waves propagating in the direction tangential to the circle of radius to maximum wind at the earlier position of the storm.

Liu (2006) have studied extensively on the sensitivity of nearshore windwaves to hurricane intensity and its translation. Their findings are pertinent to describe here. The hurricane translation speed makes a significant contribution to the asymmetric structure of the waves (Fig. 2). Furthermore, the translation speed can enhance the resultant significant wave height in the front-right quadrant of the hurricane track due to the resonance effect. This effect is significant when the hurricane translation speed increases and becomes comparable with the group speed of the dominant waves, but weak when the hurricane translation speed is much larger or less than the group speed of the dominant waves. On the other hand, it can reduce the value of the significant wave height in the rear-left quadrant of the hurricane track because of a reduction of the wind-forcing time and effective fetch. It

**Fig. 1** Schematic of swell direction with respect to storm direction

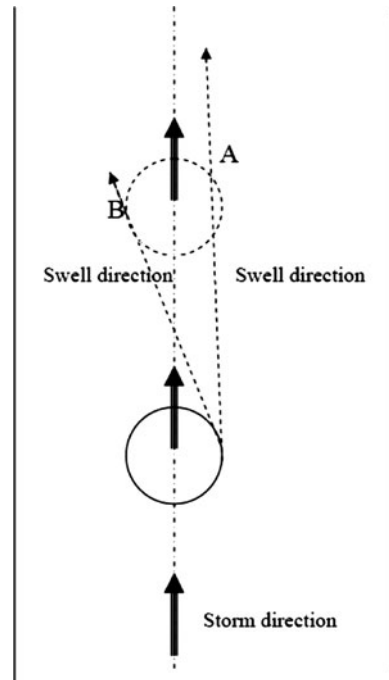
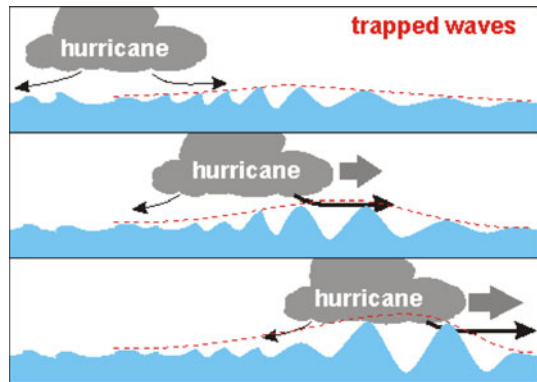


**Fig. 2** Asymmetry of waves trapped under cyclone



can contribute towards increasing wave energy, when the hurricane translation speed increases to the level comparable to the group speed of the dominant waves. The effect of hurricane intensity on waves obviously increases significant wave height with increasing wind speed or hurricane intensity. Sometimes, the hurricane translation speed causes less asymmetry for more intense hurricanes than that of weaker storms. Another factor affecting the structure of the wind-waves is the asymmetric distribution of hurricane winds. The exact asymmetric structure of a hurricane, if taken into account in wave models, it can considerably alter the significant wave height distribution and improve the quality of wind-wave prediction. The effect of prevailing wind field on waves can also significantly contribute before the effects of hurricanes come into force over the forecast domain. Thus,

the prediction of the significant wave height can be considerably improved by superimposing the prevailing wind field and the hurricane wind field. A few investigators (Fan et al. 2009a) have studied the effect of storm surge and the surge induced current on surface waves by dynamically coupling the numerical models (Kim et al. 2008). In the present study, the authors have estimated the cyclonic wind field using a well-established relationships suggested by Jelesnianski and Taylor (1973) and used as the input for SWAN wave model by one-way coupling with POM model.

### 3 One-way coupling

Multi-scale fully coupled wind-surge-current-wave ocean wave prediction system is essential to accurately forecast wave fields in shallow coastal seas during extreme wind and wave events. Successful implementation of the oceanographic models require finite difference method for regular/uniform grids or finite element method for unstructured meshes consistent with bathymetric variations over the study area. In general, the adopted approximations and the quality of these grids/meshes generated including the shape of the elements strongly influence the quality of the results of numerical simulations. It is seen worldwide that majority of operational forecast models that disseminate wave information on various websites use nested grids over uniform lengths of latitude and longitude intervals, while the research and commercial models use flexible grid mesh. The modelling packages used for coastal engineering applications also follow a hybrid approach of flexible grid mesh and uniform high-resolution grid mesh (Fig. 3). In this study, authors have demonstrated the simulation of waves following the hybrid approach utilizing the advantages of both structured and unstructured grid.

In real-world scenario, while the cyclone passes over the sea surface simultaneously generate surge-induced ocean surface current and the resultant surface waves coupled with

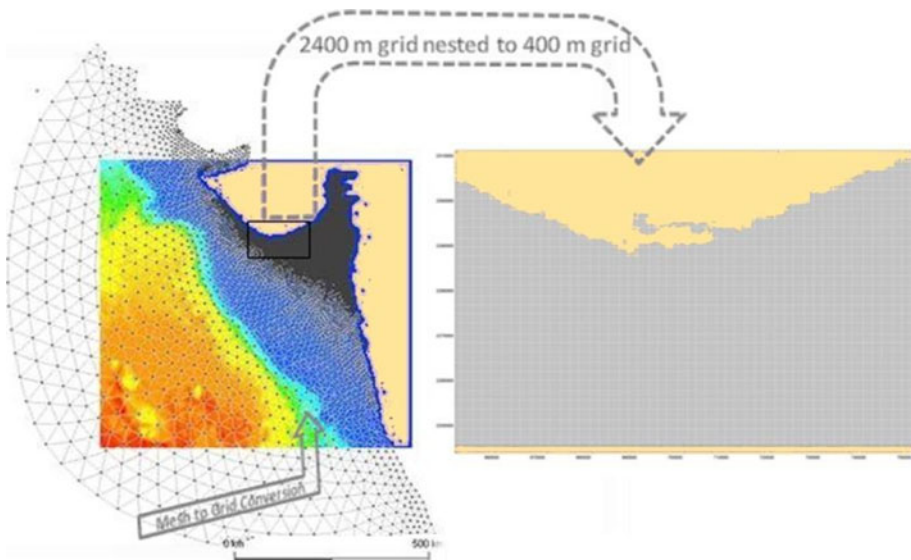


**Fig. 3** Scaling of mesh to regional grid and nesting with local grid

the low-pressure system and rapidly turning winds. Wind-generated waves, storm surge and surface current are important, mutually interacting physical processes to be simultaneously considered in predicting the surface waves. Over the past two decades, there have been a number of studies focusing on wave–current interactions (Tolman 1991; Zhang and Li 1996; Xie et al. 2001, 2003). Tolman (1991) described the effects of storm surges on evolution of waves with due consideration of unsteady currents and varying topography. The results suggest that the effects of storm surges need to be considered for predicting surface gravity waves in shallow shelf seas. Considering the importance of these interactions, there have been several studies that have attempted to incorporate these separate and linked effects that are important to take advantage out of the one-way and two-way coupled models. In these studies, storm surge and associated current are considered as the external inputs for the surface wave models. Here, the wave model and the storm surge models considered are SWAN and POM, respectively. The coupling procedure adopted in this study is one-way, i.e. currents and water elevations computed from POM are used in SWAN to integrate the evolution of two-dimensional wave spectra and the estimation of wave parameters. However, the tidal fluctuations are not considered in the present simulation experiment and the bathymetry is fixed with respect to Chart Datum (CD).

This is the first attempt by the authors to simulate waves using SWAN and POM with one-way coupling over the regional grid system in the Indian Seas by considering an extreme wind and wave event. The time-varying surge and current are provided to the wave model for every time step (but not vice versa). It would be robust and appropriate to have a two-way interactive coupling, but the present work considers one-way coupling since SWAN is implemented independent of POM over a coarser resolution in the open ocean and uses corresponding estimated cyclonic winds that may also suffer in their accuracies and lack in tidal inputs.

#### 4 Generation of cyclonic wind fields

The structure of the hurricane wind field has been the subject of considerable research (Schloemer 1954; Graham and Hudson 1960; Smith 1968; Gray and Shea 1973; Simiu et al. 1976; Atkinson and Holliday 1977; Wang 1978; Holland 1980). The vortex-shaped wind fields in these well-formed systems are relatively similar from storm to storm. This similarity makes the prediction of the wind field more reliable than in the case of less organized meteorological systems. Nevertheless, there is variability between storms, and a full understanding of the hurricane wind field is still lacking. However, the formula suggested by Jelesnianski and Taylor (1973) is used in this study for the estimation of wind fields from cyclone track data (Fig. 4). The category of cyclone and associated track information are presented in Table 1. The track data derived from satellite observations of the cyclone consist of six hourly records of position of the centre of the cyclone, estimate of the maximum wind speed as well as direction and the speed of travel for the cyclonic system. The wind speed exactly at centre of a cyclone is generally zero. Around the cyclone centre if we move outwards, wind speed increases in proportion to the distance from its centre until a maximum wind speed is reached. Further outward from the radius of maximum wind speed, the wind speed decrease exponentially. The radius of the maximum wind speed typically ranges from 20 to 50 km in the case of a severe tropical cyclone. It may be also noted that along with the changing cyclonic wind circulation, there is simultaneous movement of the whole system unless it is occasionally stationary. In this study, a wind field over a larger area of the Arabian Sea is estimated for each model time

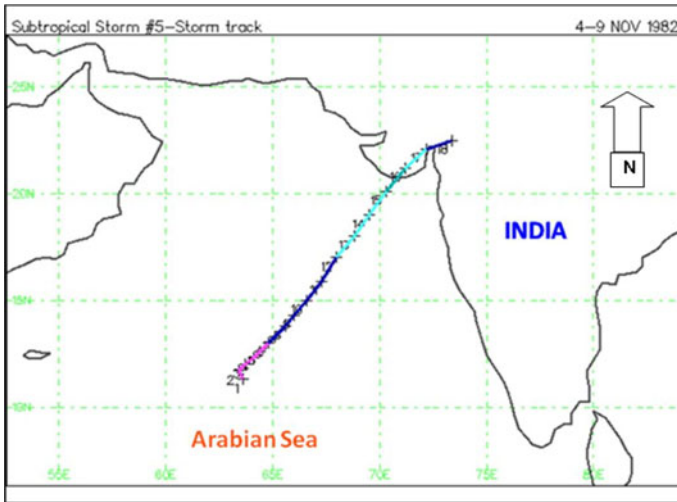


**Fig. 4** The track of the centre of 4–9 November 1982 Cyclone crossing the Arabian Sea

**Table 1** Category description for Cyclone Track as shown in Fig. 4

Type	Category	Pressure (mb)	Winds (knots)	Winds (mph)
Depression	TD	–	<34	<39
Tropical storm	TS	–	34–63	39–73
Hurricane	1	>980	64–82	74–95
Hurricane	2	965–980	83–95	96–110
Hurricane	3	945–965	96–112	111–130
Hurricane	4	920–945	113–135	131–155
Hurricane	5	<920	>135	>155

step for the whole period starting with the development and evolution of the cyclone until it disappears. A snapshot of the estimated wind field that prevailed before 1 h of cyclone land fall is shown in Fig. 5 as an example for the whole model domain used to execute the wave model at 6-h intervals. The grid resolution for the estimated wind field utilized as model input was  $2.4 \times 2.4$  km. At each location of the model grids, the wind was determined based on the recorded parameters of the cyclone for the corresponding time and distance from the cyclonic centre as per the Jelesniaski and Taylor’s formula:

$$U_i = \frac{2rR_{\max}}{r^2 + R_{\max}^2} U_{\max} \tag{1}$$

where  $U_i$  is the speed (m/s) at location  $i$ ,  $r$  is the distance (m) from the centre of the cyclone,  $U_{\max}$  is the maximum wind speed (m/s) and  $R_{\max}$  is the radius (m) of the maximum wind speed. The wind direction is assumed to be at right angles to the line joining the grid location and the centre point of the eye of the cyclone i.e. a circular wind pattern. In general, the wind circulation is anticlockwise for the cyclones in the northern hemisphere. Wind speed is higher on that side of the cyclone where the cyclone wind circulation is in the same direction as that of the systemic velocity. The method of estimating cyclone



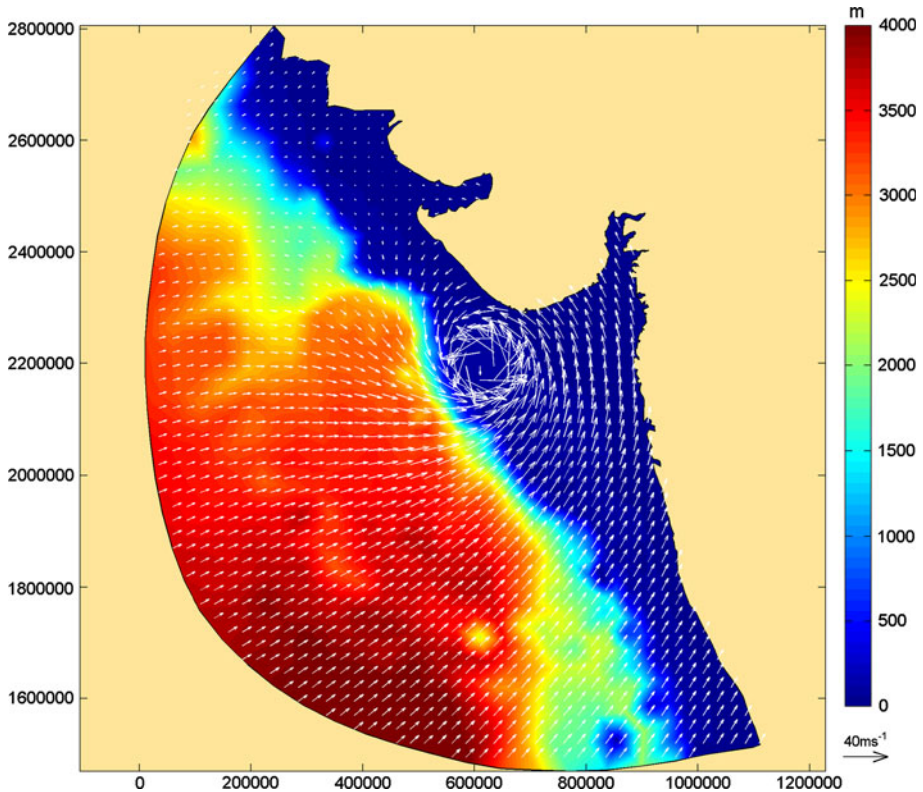


**Fig. 5** Bathymetry for SWAN model and simulated wind fields (shown with sticks) 1 h before land fall

winds in this study is of course a simplified approach compared with the real-world scenario, as the wind field around a cyclone is considered much more complex. In this particular case study, the winds over the land as well as sea were considerably strong even after the cyclone land fall.

## 5 Sea surface hydrodynamics during cyclone

The hydrodynamics of the ocean surface during the cyclone event is simulated using POM. POM model originally was developed by Blumberg and Mellor (1987). The model is widely used for predicting coastal currents and water surface elevations. It includes thermodynamic processes, turbulent mixing, the Boussinesq and hydrostatic approximations. The Coriolis parameter is allowed to vary using beta-plane approximation. Since the model includes a wide range of water depths (m) of the region considered, Blumberg and Mellor used a vertical coordinate system scaled by the depth of the water:

$$\sigma = \frac{Z - \eta}{H + \eta} \quad (2)$$

where  $z = \eta(x, y, t)$  is the sea surface, and  $z = -H(x, y)$  is the sea bottom.



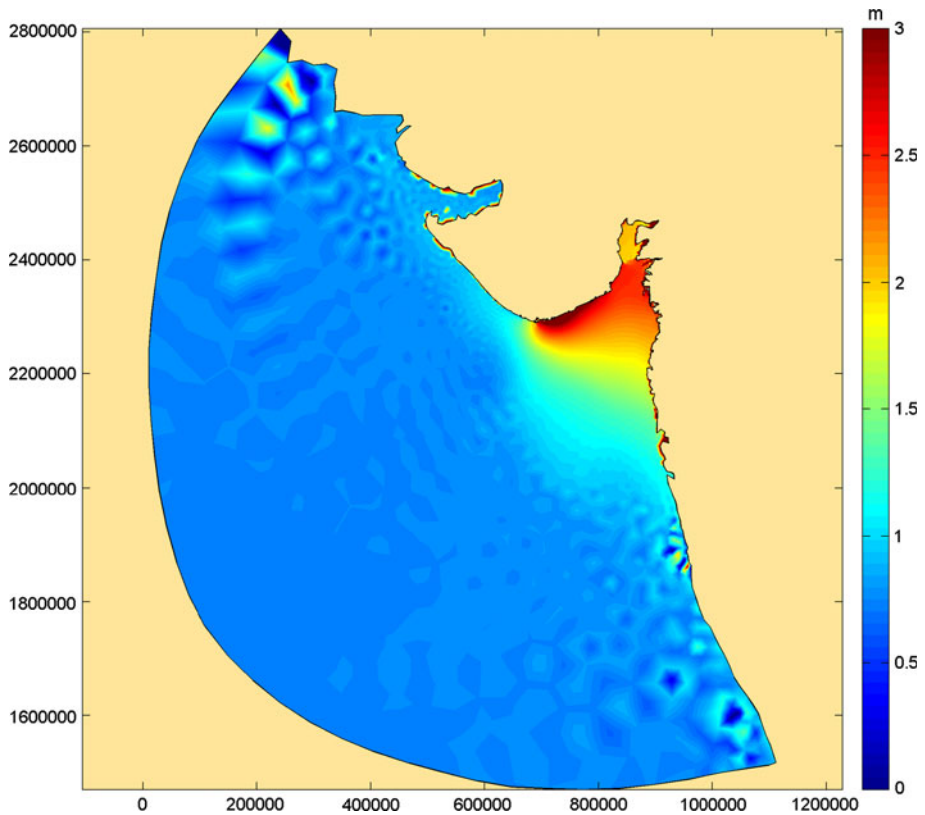


**Fig. 6** POM-Simulated storm surge 1 h before land fall

Sub-grid turbulence is parameterized using a closure scheme proposed by Mellor and Yamada (1982) whereby eddy diffusion coefficients vary with the size of the eddies producing the mixing and shear flow. The model is driven primarily by estimated wind stress as well as heat and water fluxes as input from the operational weather prediction model analysis. Further inputs considered for the simulation are the known geostrophic, tidal and Ekman currents along the boundaries of the model domain considered. The simulated POM outputs of storm surge and surface current are presented in Figs. 6 and 7 for the corresponding wind input time step, an hour before the land fall of cyclone.

## 6 Simulation of waves during cyclone

Wind-generated waves are the most predominant nearshore activity that generate long-shore currents and transport sediments by re-shaping coastal zone. They can be predicted over extensive areas such as the global and regional oceans, seas and shelf areas, which is practically feasible using state-of-the-art numerical models in single or multiple phases. Numerical wave models are based on the principle of spectral energy balance, with linear/curve-linear wave propagation and a set of source terms which account for wind input,

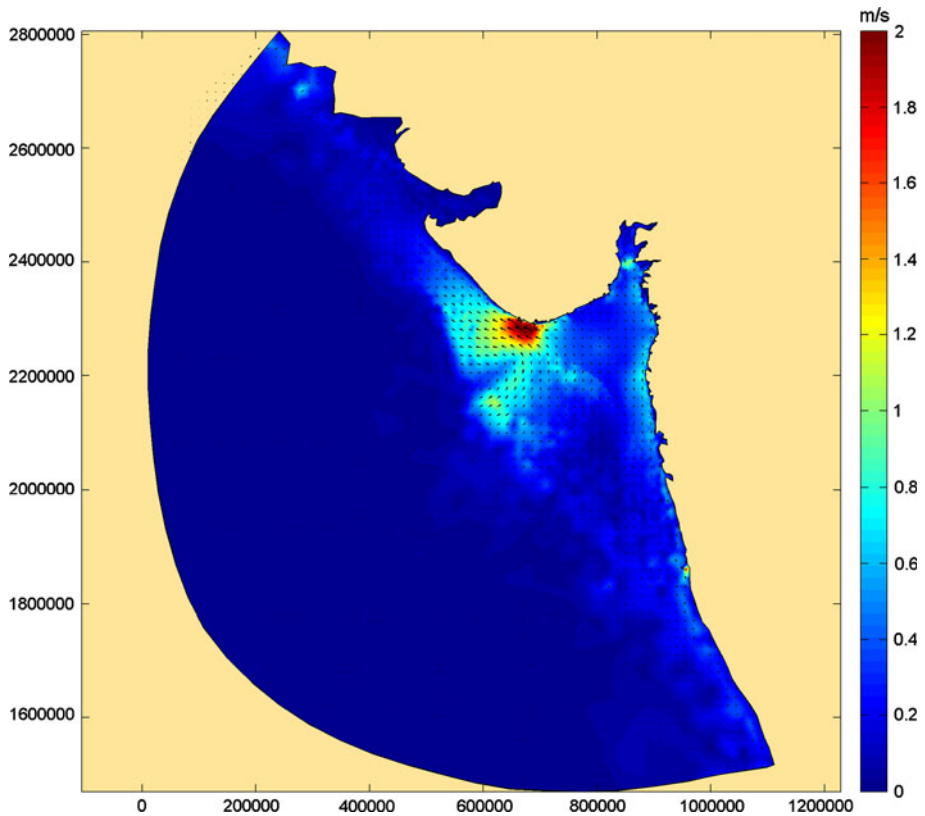


**Fig. 7** POM-simulated current 1 h before land fall

cross-spectral transfer and dissipation. The first wave model in this category is WAM developed for deep water, with some allowances for restricted water depth up to 30 m. WAVEWATCH III (WWIII, Tolman 1991) is a similar model developed subsequently incorporating latest physics and numerical schemes. Yet another model SWAN used in this study is based on the similar principles of WAM and WWIII, which is designed especially for shallow coastal regions (Booij et al. 1999) as an extension of the deep-water models. The prediction skill of these models has been widely demonstrated by various researchers with the use of measured data from satellites, buoys and other platforms.

SWAN model is based on the wave action balance equation with sources and sinks. In this model, evolution of wave spectrum is described by the spectral action balance equation as shown below:

$$\frac{\partial}{\partial t} N + \frac{\partial}{\partial x} C_x N + \frac{\partial}{\partial y} C_y N + \frac{\partial}{\partial \sigma} C_\sigma N + \frac{\partial}{\partial \theta} C_\theta N = \frac{S}{\sigma} \quad (3)$$

where  $N$  is the action density ( $N(\sigma, \theta) = E(\sigma, \theta)/\sigma$ ),  $E$  is the energy density spectrum and  $\sigma$  is the relative frequency.  $C_x$ ,  $C_y$ ,  $C_\sigma$  and  $C_\theta$  are propagation velocities in  $x$ -,  $y$ -,  $\sigma$ - and  $\theta$ -space, respectively.  $S$  is the source term that represents the effects of generation, dissipation and nonlinear wave–wave interactions. The term at the right-hand side of the

wave action balance equation is the source term of energy density representing wave generation due to wind, non-linear wave–wave interactions and energy dissipation as given below:

$$S = S_{in} + S_{nl} + S_{ds} \tag{4}$$

$S_{in}$  is the energy input from the wind. The three processes for energy dissipation ( $S_{ds}$ ) are white capping, bottom friction and depth-induced wave breaking where bottom friction dominates in shallow waters, whereas white capping is the main source of energy dissipation in deep waters. Energy is transformed between waves through nonlinear wave–wave interactions ( $S_{nl}$ ). In shallow waters, triad wave–wave interactions play a major role. However, quadruplet wave–wave interactions are considered as enough for the deep waters. In this study, all default values of physical parameters in the SWAN model are adopted since the primary objectives of this study is to evaluate the feasibility and applicability of SWAN for cyclonic waves in the region of study. SWAN-simulated wave height ( $H_s$ ) distribution and period ( $T_m$ ) along with mean wave direction right under the eye of the cyclone in deep water is presented in Figs. 8 and 9. Similarly, the nearshore wind fields, surge level, wave height, wave period and direction are plotted in Figs. 10a, b, 11a and b, respectively, right at the time of land fall point.

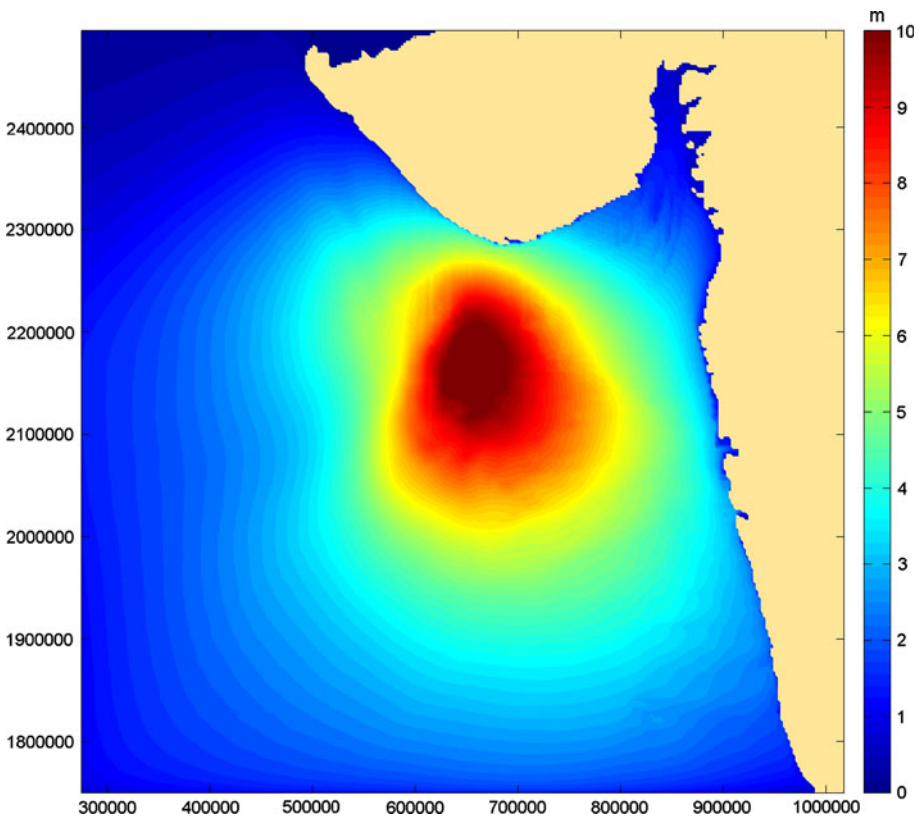


**Fig. 8** SWAN-simulated significant wave height (m) 1 h before land fall

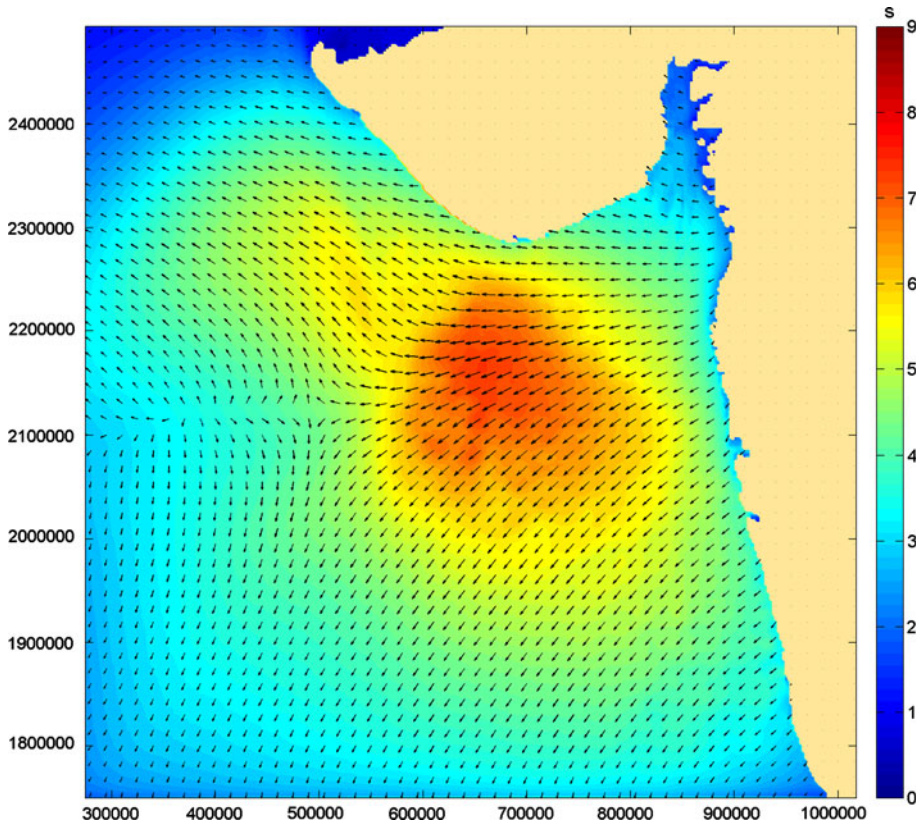


**Fig. 9** SWAN-simulated mean wave period (s) and direction (deg.) 1 h before land fall

## 7 Results and discussion

As stated earlier, by utilizing the historical record of cyclone track obtained from UNISYS and the methodology described in the Sect. 4, the cyclonic wind fields were estimated for the simulation of cyclonic wave conditions to the best possible extent. The cyclone lasted for nearly 6 days from 1,800 h of 4th November to 00 h of 9th November 1982 in the Arabian Sea as shown in Fig. 4, and the maximum wind speed had reached up to 155 km/h. The cyclonic wind fields that were estimated from track records at 1,800 s interval for the whole period of cyclone up to 6 h of land fall could reasonably predict the evolution of wave field. The Arabian Sea bathymetry, which was prepared combining ETOPO data set (National Geophysical Data Center 2006) for deep sea region and CMAP data set (Jeppesen Marine) for shallow waters for nearshore simulation as indicated earlier were found to be realistic for the present study. The turning wind field over the study region that corresponds to an hour before the land fall of cyclone (Fig. 5) is in agreement with the re-analysis wind fields reported by various operational agencies. Model simulations were continued until 6 h of cyclone land fall as the winds were strong enough for the evolution of waves near shore. Therefore, the model results have been plotted and analysed accordingly for the predicted fields 1 h before land fall for deep water domain (2,400 m) and right at land fall time for shallow water domain (400 m).

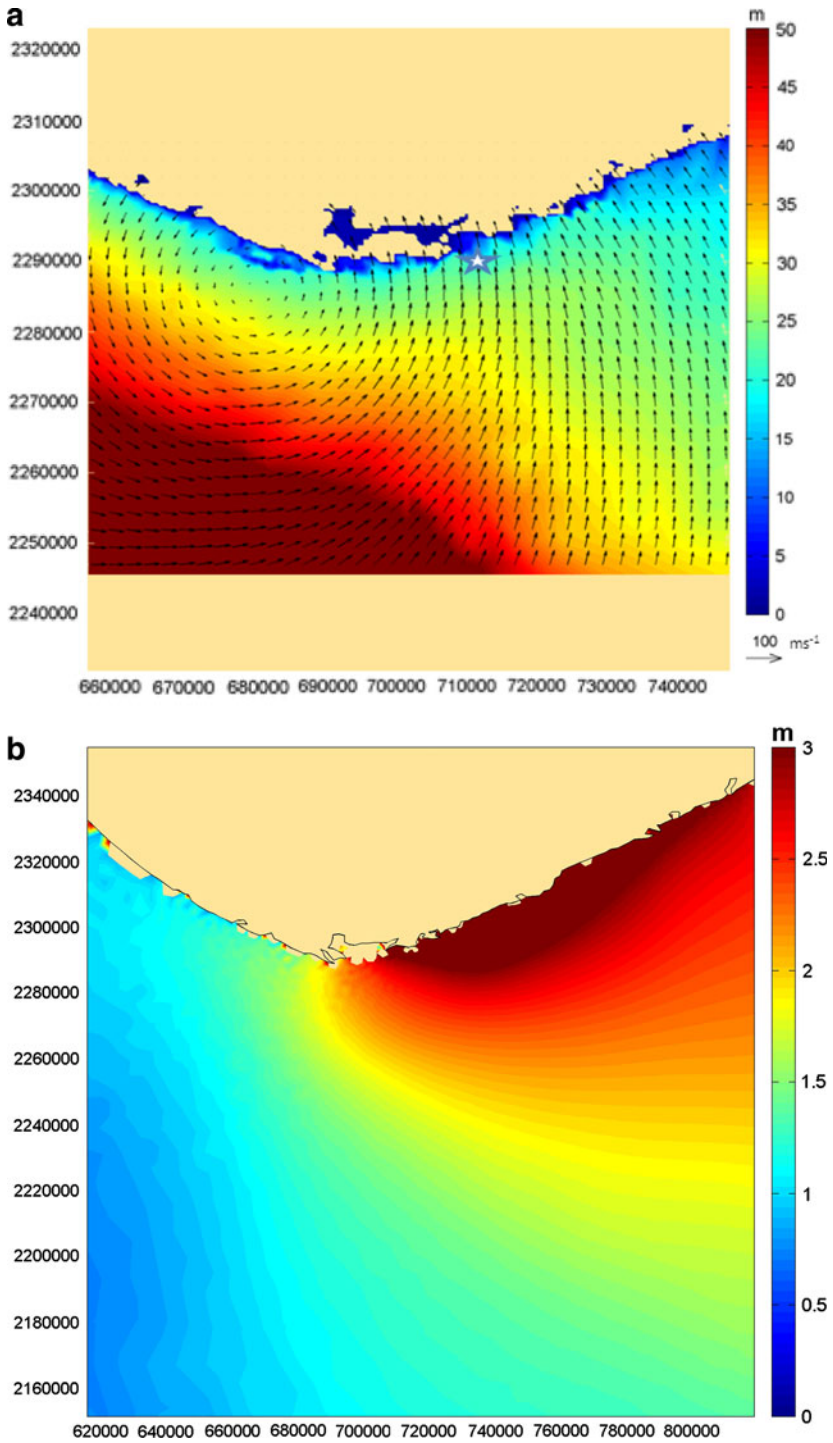


**Fig. 10** a Nearshore SWAN domain and wind fields right at land fall. b Nearshore storm surge right at land fall



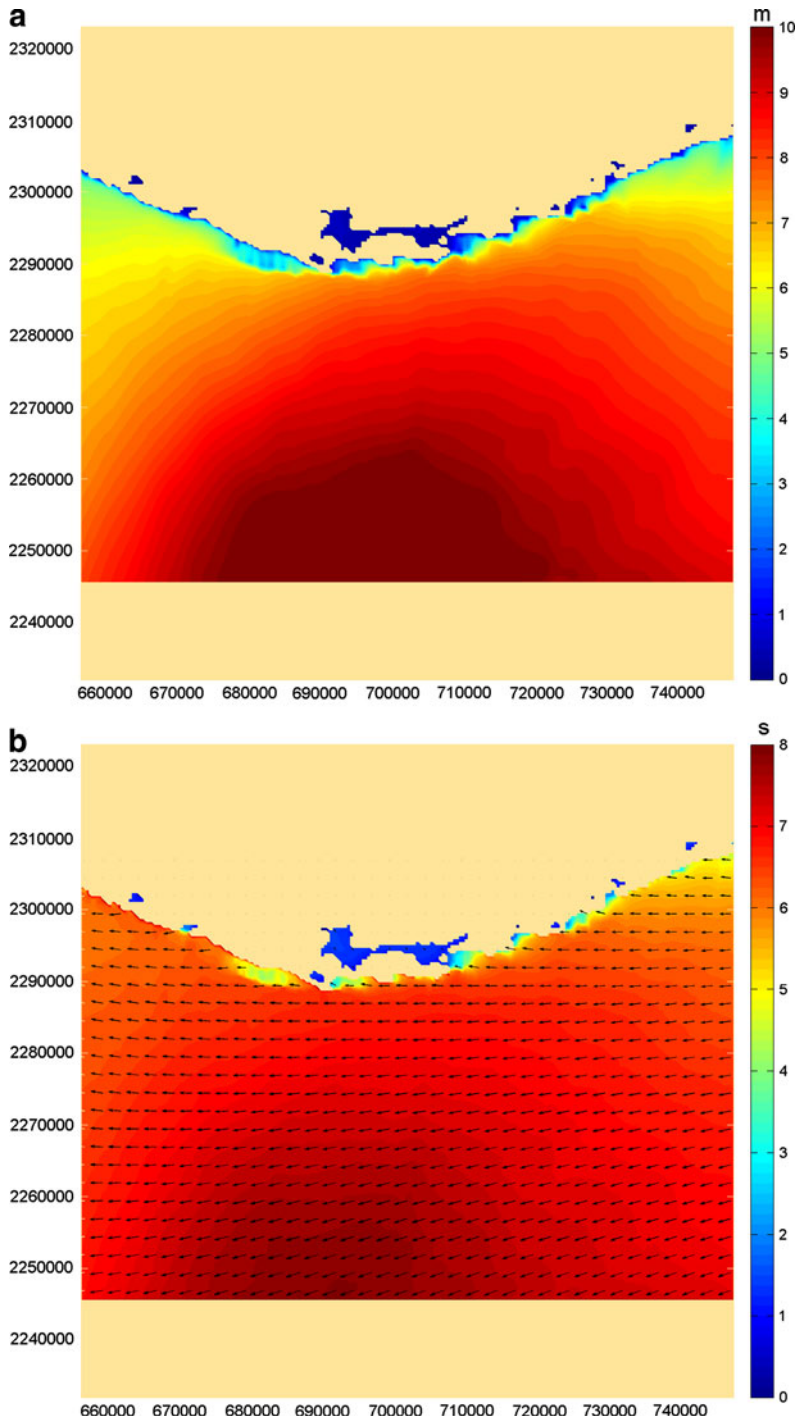


**Fig. 11** **a** Nearshore wave height ( $H_s$ ) right at land fall. **b** Nearshore wave period ( $T_m$ ) and mean wave directions right at land fall

The POM model, which was executed with 900 s source integration time steps utilizing the estimated wind fields along the track of the cyclone could reasonably simulate the surge levels and the associated surface currents. The storm induced surge and associated current pattern an 1 h before the cyclone land fall presented in Figs. 6 and 7 are quite encouraging. It may be seen that a surge of the order of 3.0 m over CD was generated by the low-pressure system of the cyclone off the southern coast of Gujarat. Similarly, the surge elevation associated with wind stress could reproduce a strong current of the order of 2.0 m/s along the coast. Such a strong current due to storm surge is the result of wind shear stress and the barometric pressure gradients over the entire oceanic region influenced by the storm. The horizontal current velocity profile as predicted by POM appeared to follow a logarithmic distribution similar to the tidal current. The simulated results reveal that the current strength is stronger towards deeper waters (Figs. 6, 7) away from the coastline and in confined areas such as straits and tidal inlets. Further, it may be seen from Figs. 6 and 7 that the direction of current is opposite to direction of surge propagation. This suggests that as the water piles up due to the rise in surge level, it induces sub-surface flow of water to the surrounding areas.

The hydrodynamic results such as the surge levels and currents used as input for subsequent simulation of waves offshore and nearshore as explained before have shown their significant impact as compared to the results obtained without the surge level and current input. Therefore, SWAN executions that were carried out using estimated winds and water surface variations due to surge and surface induced resultant current by considering an integration time step of 900 s throughout the period of cyclone revealed to be most appropriate in simulating the cyclone wave evolution for the region of interest. However, the results could not be validated due to the unavailability of measured data. The wave height distribution presented in the Fig. 8 corresponds to 1 h before the cyclone land fall and shows intense wave activities somewhat away from the eye of the cyclone. The spatial distribution of waves show an interesting circular pattern of propagating waves as high as 10.0 m, which is the peak wave height at the central region, more or less comes under the cyclone track. The mean wave period varied between 5 and 8 s (Fig. 9) around the cyclone land fall, which reveal that the sea-state is composed of combined wind-seas and swells due to the changing as well as rotating of the cyclone winds. Further, it is quite interesting to see from Fig. 9 that the waves are propagating offshore and in varying directions (NW and SW) in the surrounding regions of the cyclone track. It contradicts with the schematic 1 and 2 presented in literature review Sect. 2. The general assumptions on wave direction with respect to storm track suggested by Young (1988) could not justify. The authors account this with the facts (Fan et al. 2009a, b) that the simplification of the wind formulation without considering asymmetry of the cyclone and effect of the coastal wind i.e. land influence to cyclone wind.

The nearshore wind, surge distributions, SWAN-predicted wave heights and period along with mean wave direction right at the land fall time are shown in Figs. 10a, b, 11a and b, respectively. It reveals the severity of the cyclone at land fall point. It is well known that the simulated parameters of wave and surge in shallow waters are most important for coastal engineers. Therefore, from their application point of view, highest occurrences of storm surge, wave height ( $H_{m0}$ ), wave period ( $T_m$ ) and wave direction parameters at 5, 10, 15 and 20 m CD contours have been extracted from a nearby region of the cyclone land fall and presented in Table 2. As a typical example, the table reveals that the November 1982 cyclone has contributed a surge height of 3.0 m, significant wave height of 5.0 m and mean wave period of 6.2 s propagating from ESE quadrant at 10 m water depth. Similarly, at 20 m water depth, the surge height, significant wave height, mean wave period and wave



**Table 2** Shallow water surge and wave characteristics

Depth (CD) (m)	Surge level (m)	Hm <sub>0</sub> (m)	Tm (s)	Direction (deg.)
5.0	3.1	3.6	5.9	97.2
10.0	3.0	5.0	6.2	100.5
15.0	2.9	6.3	6.1	94.3
20.0	2.8	7.6	6.6	84.4

direction parameters are predicted as 2.8, 7.6 m, 6.6 s and 85°, respectively. The values of said parameters are more or less comparable at 10 and 20 m water depths excepting a significant wave height reduction of 2.5 at 10 m water depth compared to 20 m water depth.

In this case study, the predicted wave spectra of SWAN at nearshore region were predominantly single peaked indicating a strong coupling between the cyclone winds and the resultant waves as the cyclone track coincided with the propagating waves from off-shore to nearshore waters off Gujarat. A typical wave energy spectrum from a selected point (indicated as star in Fig. 10a) in the study area at 10 m CD is shown in Fig. 12. The spectra reveal that the SWAN-predicted energy spectrum against selected frequencies compare well with the theoretical Peirson–Moskowitz spectrum along with the corresponding peak periods and significant wave heights as well. As both these wave spectra compare well with each other, they clearly indicate that the waves or the prevailing sea-state due to the cyclonic storm was more or less fully developed as the cyclone lasted long (Hasselmann et al. 1973).

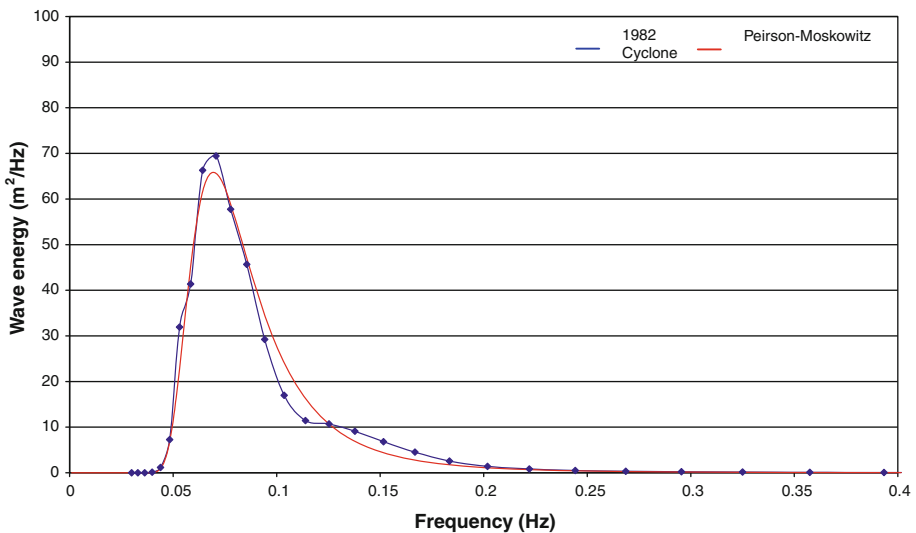


**Fig. 12** A typical wave energy spectrum at 10 m depth from SWAN and equivalent Peirson–Moskowitz spectrum for the same significant wave height and peak period

## 8 Summary and conclusion

The study is an useful exercise for the prediction of cyclonic waves for the north-west coast of India (off Gujarat) with the use of a third generation spectral wave model SWAN using empirically estimated winds based on the cyclone track records. The unique contribution of this study is the wave evolution incorporating the two important hydrodynamic parameters such as the storm surge levels and surface current that were simulated using POM. The one-way coupling approach using POM and SWAN is quite promising in predicting the extreme wave height due to the complex cyclonic wind fields. The results presented in this paper confirm that a fully coupled wind-wave-surge-current-ocean modelling system as suggested by Fan et al. (2009a) is necessary to predict wave fields during extreme weather conditions more accurately. The primary limitation of the present study is the unavailability of measured data during the passage of the cyclone for validation of simulated wave fields. The simulated storm wave direction seems to be nebulous and deviate from normal convention, which may need further studies to confirm. Secondly, the present study lack in the tidal input, which could have further enhanced predictions of waves nearshore. In general, the head land of Gujarat is the landfall point for a number of cyclones generated in the Arabian Sea. Therefore, it would demand further research to ascertain the role of head land on diverging wave direction. By and large, the authors have demonstrated the usefulness of storm surge, associated currents during the cyclone event in simulating wave characteristics in shallow water for a high-resolution model domain. This study is useful for various coastal engineering applications including the development and up-keep of minor ports and maritime structures around the site.

**Acknowledgments** The present study is an extension of Dr. Jitendra K. Panigrahi's Doctoral research work at Naval Physical and Oceanographic Laboratory, Cochin on deepwater waves (WAM) to shallow waters using SWAN at Department of Marine Science, Berhampur University, India. The authors gratefully acknowledge Delft University of Technology and Princeton University for providing the state-of-art SWAN and POM model, respectively, in World Wide Web.

## References

- Atkinson GD, Holliday CR (1977) Tropical cyclone minimum sea level pressure- maximum sustained wind relationship for western North Pacific. *Mon Weather Rev* 105:421–427
- Blumberg A, Mellor GL (1987) A description of a three-dimensional coastal ocean circulation model. In: Heaps NS (ed) *Three-dimensional coastal ocean models*. American Geophysical Union, Washington, DC, pp 1–16
- Booij N, Ris RC, Hothuijsen LH (1999) A third-generation wave model for coastal regions: model description and validation. *J Geophys Res* 104(c4):7649–7666
- ETOPO (2006) National geophysical data center, 2-minute gridded global relief data (ETOPO2v2), National Oceanic and Atmospheric Administration. US Dept. of Commerce (<http://www.ngdc.noaa.gov/mgg/fliers/06mgg01.html>)
- Fan Y, Ginis I, Hara T (2009a) The effect of wind-wave-current interaction on air-sea momentum fluxes and ocean response in tropical cyclones. *J Phys Oceanogr* 39:1019–1034
- Fan Y, Ginis I, Hara T, Wright CW, Walsh E (2009b) Numerical simulations and observations of surface wave fields under an extreme tropical cyclone. *J Phys Oceanogr* 39:2097–2116
- Graham HE, Hudson GN (1960) Surface winds near the center of hurricanes (and other cyclones). NHRP Rep. Govt. Print Office 39, 200
- Gray WM, Shea DJ (1973) The hurricane's inner core region II: thermal stability and dynamic characteristics. *J Atmos Sci* 30:1565–1576
- Hasselmann K, Barnett TP, Bouws E, Carlson H, Cartwright DE, Enke K, Ewing JA, Gienapp H, Hasselmann DE, Kruseman P, Meerburg A, Muller P, Olbers DJ, Richter K, Sell W, Walden H (1973)

- Measurements of wind-wave growth and swell decay during the Joint North Sea Wave Project (JONSWAP). *Dtsch Hydrogr Z* 12:A8
- Holland GJ (1980) An analytical model of the wind and pressure profiles in hurricanes. *Mon Weather Rev* 108:1212–1218
- Jelesnianski CP, Taylor AD (1973) A preliminary view of storm surges before and after storm modifications. NOAA Technical Memorandum ERL WMPO-3, Washington, DC, pp 23–33
- Kim KO, Yamashita T, Choi BH (2008) Coupled process-based cyclone surge simulation for the Bay of Bengal. *Ocean Model* 25:132–143
- Komen GJ, Cavaleri L, Donelan M, Hasselmann K, Hasselmann S, Janssen PAEM (1994) Dynamics and modelling of ocean waves. Cambridge University Press, New York
- Liu H (2006) Analysis and modeling of wave-current interaction. Ph.D. thesis, North Carolina State University. Chapter-4, pp 73–104
- Mellor GL (1996) Users guide for a three dimensional, primitive equation numerical ocean model. Princeton University Press, Princeton
- Mellor GL, Yamada T (1982) Development of a turbulence closure model for geophysical fluid problems. *Rev Geophys Space Phys* 20:851–875
- Miles JW (1957) On the generation of surface waves by shear flows. *J Fluid Mech* 3:185–204
- Moon IJ, Ginis I, Hara T, Tolman HL, Wright CW, Walsh EJ (2003) Numerical simulation of sea surface directional wave spectra under hurricane wind forcing. *J Phys Oceanogr* 33:1680–1760
- Moon IJ, Ginis I, Hara T (2004) Effect of surface waves on air-sea momentum exchange. Part II: behavior of drag coefficient under tropical cyclones. *J Atmos Sci* 61:2334–2348
- Ou S-H, Liau J-M, Hsu T-W, Tzang S-Y (2002) Simulating typhoon waves by SWAN wave model in coastal waters of Taiwan. *Ocean Eng* 29:947–971
- Panigrahi JK, Misra SK (2009) Numerical hindcast of extreme waves. *Natl Hazards*. doi:[10.1007/s11069-009-9438-4](https://doi.org/10.1007/s11069-009-9438-4)
- Phillips OM (1957) On the generation of waves by turbulent wind. *J Fluid Mech* 27:4815–4827
- Ris RC, Holthuijsen LH, Booij N (1999) A third-generation wave model for coastal regions, 2. Verification. *J Geophys Res* 104(C4):7667–7681
- Schloemer RW (1954) Analysis and synthesis of hurricane wind patterns over lake Okechobee. FL Hydromet Report, Govt. Print Office, pp 31–49
- Simiu E, Patel VC, Nash JF (1976) Mean speed profiles of hurricane winds. *J Eng Mech ASCE* 102:265–273
- Smith RK (1968) The surface boundary layer of a hurricane. *Tellus* 20:473–484
- Tolman HL (1991) Effects of tides and storm surges on North Sea wind waves. *J Phys Oceanogr* 21:766–781
- Walsh EJ, Wright CW, Vandemark D, Krabil WB, Garcia AW, Houston SH, Murillo ST, Powell MD, Black PG, Marks FD (2002) Hurricane directional wave spectrum spatial variation at landfall. *J Phys Oceanogr* 32:1667–1684
- WAMDI group (1988) The WAM model—a third generation ocean wave prediction model. *J Phys Oceanogr* 18:1775–1810
- Wang GC (1978) Sea level pressure profile and gusts within a typhoon circulation. *Mon Weather Rev* 106:954–960
- Wang DW, Mitchell DA, Teague WJ, Jarosz E, Hulbert MS (2005) Extreme waves under Hurricane Ivan. *Science* 309:896
- Wright CW, Walsh EJ, Vandemark D, Krabil WB, Garcia AW, Houston SH, Powell MD, Black PG, Marks FD (2001) Hurricane directional wave spectrum spatial variation in the open ocean. *J Phys Oceanogr* 31:2472–2488
- Xie L, Wu K, Pietrafesa LJ, Zhang C (2001) A numerical study of wave-current interaction through surface and bottom stresses: wind-driven circulation in the South Atlantic Bight under uniform winds. *J Geophys Res* 106:16841–16855
- Xie L, Pietrafesa LJ, Wu K (2003) A numerical study of wave-current interaction through surface and bottom stresses: Coastal ocean response to Hurricane Fran of 1996. *J Geophys Res* 108(C2):3049–3167
- Young IR (1988) A parametric hurricane wave prediction model. *J Waterw Port Coast Ocean Eng ASCE* 114(5):637–652
- Young IR (2006) Directional spectra of hurricane wind waves. *J Geophys Res* 111(C8):C08020. doi:[10.1029/2006JC003540](https://doi.org/10.1029/2006JC003540)
- Zhang MY, Li YS (1996) The synchronous coupling of a third-generation wave model and a two-dimensional storm surge model. *Ocean Eng* 6:533–543